ARTICLE

OBC

www.rsc.org/obc

Self-assembly and stability of double rosette nanostructures with biological functionalities†

Mattijs G. J. ten Cate, Merdan Omerović, Gennady V. Oshovsky, Mercedes Crego-Calama* and David N. Reinhoudt*

Laboratory of Supramolecular Chemistry and Technology, MESA+ Institute for Nanotechnology, University of Twente, P.O. Box 217, 7500, AE Enschede, The Netherlands. E-mail: m.cregocalama@utwente.nl; Fax: +31 53 489 4645; Tel: +31 53 489 2978

Received 15th June 2005, Accepted 2nd August 2005
First published as an Advance Article on the web 24th August 2005

The syntheses of calix[4]arene dimelamines that are functionalized with alkyl, aminoalkyl, ureido, pyridyl, carbohydrate, amino acid and peptide functionalities, and their self-assembly with barbituric acid or cyanuric acid derivatives into well-defined hydrogen-bonded nanostructures are described. The thermodynamic stability of these hydrogen-bonded assemblies was studied by CD spectroscopy in mixtures of $CHCl_3$ and MeOH. The stability of the assemblies depends on several steric factors and the polarity of the functional groups connected to the assembly components.

Introduction

Natural receptors exhibit extraordinary high binding affinity and selectivity for a particular substrate. The binding affinity and selectivity arises from the cooperative action of many chain functionalities oriented in a *three-dimensional* fashion around the target molecule.

In general, a rational-based design of synthetic molecules is used to mimic the binding properties of natural receptors. However, large covalent systems are difficult to synthesize and structural diversity can only be introduced into the scaffolds at the expense of challenging and time consuming synthesis. Therefore, self-assembly of nanostructures using multiple weak *noncovalent* interactions is considered a powerful tool for the understanding, modelling, and mimicking of biological systems.[1] A major advantage is that self-assembled structures are generally formed under thermodynamically controlled conditions, often giving rise to quantitative yields of product.[2]

The concave 3D positioning of different functionalities around a central cavity by self-assembly provides the basis for natural receptors to bind substrates and to catalyze biochemical transformations with exquisite regio- and stereoselectivity. Natural antibodies provide a perfect example of self-assembled receptors. They consist of four different peptide chains, two heavy (H) and two light (L) chains which are held together mainly by noncovalent interactions, reinforced by covalent disulfide bonds.[3] Natural antibodies have a hypervariable region (Fab) and a constant region (Fc). Because differences between antibodies arise from differences in the Fab fragments, it is not surprising that specific antigen recognition sites are located in this part of the antibody. Such self-assembled systems provide nature with a powerful tool to generate many different antibodies.

For the design of synthetic receptors, a strategy was developed in our group that is similar to the assembly of antibodies.[4] This approach involves the formation of a synthetic self-assembling platform in which a double rosette motif (constant region) is formed based on multiple hydrogen bonds (Fig. 1).[5] Functionalization of the individual components with small functional groups (X or Y in Fig. 1) gives noncovalent assemblies with diverse molecular fragments generating a potential 3D-guest-binding region (variable region). Furthermore, to mimic natural antibodies structural diversity has to be introduced to the double rosette assemblies. Structural diversity in the guest-binding region of these synthetic receptors can be generated both at a covalent level (variation in functional groups) and at a supramolecular level (statistical combination of fixed number of molecular components, Fig. 1).

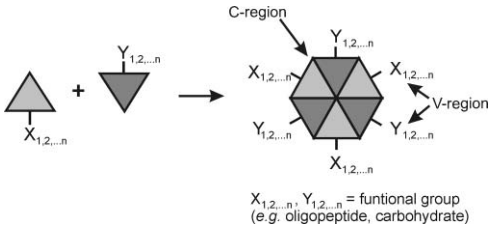

Fig. 1 Self-assembly of small functional groups *via* synthetic self-assembled platforms (rosettes).

In general, a major drawback in the use of hydrogen-bonded supramolecular systems is their low stability in polar solvents, because these solvents compete with the hydrogen-bonding motif that holds the system together. On the other hand, natural host–guest recognition events take place in aqueous environments or at the cell membranes. Therefore, the study of the formation and the stability of self-assembled hydrogen bonded systems in polar solvents is very important for the understanding and the mimicking of natural systems.

Here, we focus on the formation and stability of differently functionalized hydrogen-bonded assemblies in competitive solvent mixtures of different polarity. Both steric hindrance induced by linear or branched alkyl chains and the effect of simple polar functionalities, such as amino alkyl, ureido, and pyridyl moieties on the stability of double rosettes are investigated. Subsequently, the stability of more complex assemblies bearing sugars, amino acids or small peptide fragments is examined.

Results and discussion

The thermodynamic stability of the designed double rosette assemblies (Fig. 2) might be affected when different functionalities are introduced in the building blocks. For example, hydrogen bond donating or accepting groups can possibly interfere with the rosette platform formation, while bulky groups can cause steric strain in the assembly and decrease their thermodynamic stability.[6]

† Electronic supplementary information (ESI) available: experimental procedures and compound characterization. See http://dx.doi.org/10.1039/b508449k

DOI:10.1039/b508449k

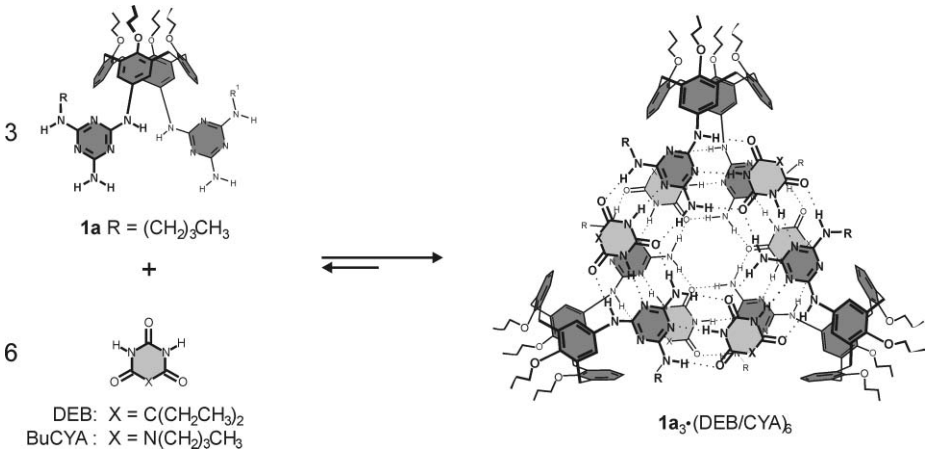

Fig. 2 Formation of the double rosette assemblies $\mathbf{1a}_3\cdot(\mathrm{DEB/BuCYA})_6$ from three calix[4]arene dimelamines **1a** and six 5,5-diethylbarbiturate (DEB) or *n*-butyl cyanurate (BuCYA) molecules.

The double rosette assemblies with dimensions of *ca.* 3.0 × 3.3 × 1.2 nm are formed spontaneously by mixing of calix[4]arenes diametrically substituted at the upper rim with two melamine units (for example **1a**, Fig. 2) with 2 equivalents of either barbituric acid (BAR) or cyanuric acid (CYA) derivatives. The assemblies $\mathbf{1}_3\cdot(\mathrm{DEB/CYA})_6$ consist of two rosette motifs,[7] connected *via* three calix[4]arene molecules. The assemblies are held together by 36 hydrogen bonds and are stable in apolar solvents like chloroform, benzene and toluene even at 10^{-4} M.[5a,8]

With the aim to generate stable and structural diverse double rosettes, calix[4]arene dimelamines bearing alkyl (**1a**–**c**), aminoalkyl (**2a**–**g**), ureido (**3**), pyridyl (**4a**–**c**), sugar (**5a**–**e**), amino acid (**6a**–**f**), dipeptide (**7a**–**e**), and tripeptide (**8a**–**b**) functionalities were synthesized (Chart 1). Subsequently, the thermodynamic stability of the corresponding rosette with these dimelamines was determined after their self-assembly with DEB, BuCYA, BzCYA, (*R*)-PhEtCYA or (*S*)-PhEtCYA in a mixture of chloroform and an increasing percentage of a competing solvent for hydrogen bonding.

Synthesis and characterization of assemblies with different functionalities

Compounds **1**–**8** were synthesized starting from calix[4]arene bis(chlorotriazine) **9**.[8] Dimelamines **2** were synthesized by reaction of **9** with an excess of the corresponding diaminoalkane at 90 °C (**2a**–**g**, 53–92%). Reaction of **2g** with excess of propyl isocyanate in THF at room temperature afforded dimelamine **3** (78%).[9] Syntheses of dimelamines **4** are described elsewhere.[10]

Reaction of **2g** with tetra-*O*-acetyl-β-D-glucopyranosyl-isothiocyanate and hepta-*O*-acetyl-β-D-cellobiosyl-isothiocyanate[11] in THF gave dimelamines **5a** (36%) and **5c** (88%), respectively. Successive deacetylation of **5a** and **5c** with a catalytic amount of a sodium methoxide solution afforded dimelamines **5b** and **5d**, respectively. Compound **5e** was obtained in 41% yield by coupling of **2g** and gulonic acid with HBTU in the presence of HOBT and DIPEA in CH_2Cl_2 at room temperature.

Dimelamines **6a**–**d** were obtained by reaction of **9** with excess of glycine ethyl ester (**6a**, 74%), L-alanine methyl ester (**6b**, 74%), L-methionone methyl ester (**6c**, 69%), or L-lysine(Boc) methyl

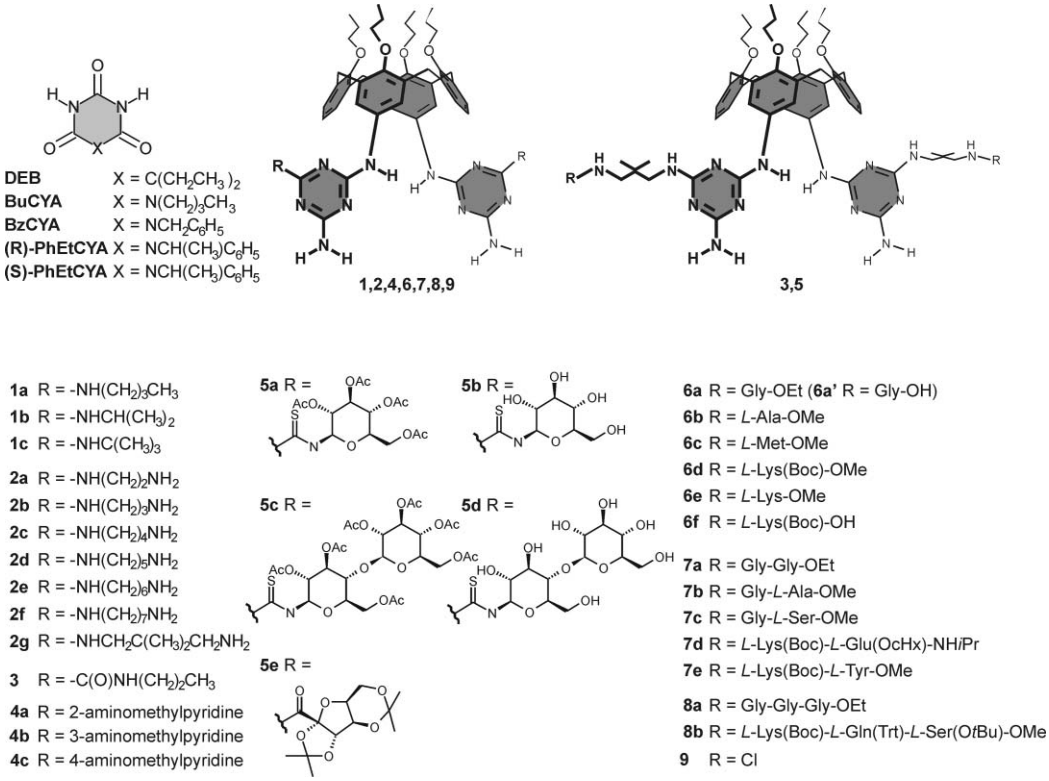

Chart 1 Molecular structures of dimelamines **1**–**9** and BAR/CYA derivatives.

ester (**6d**, 84%) in presence of DIPEA in THF. Deprotection of the ε-amino group of dimelamine **6d** with TFA–CH_2Cl_2 (1 : 1) afforded compound **6e** in 24% yield. Hydrolysis of compound **6d** with sodium hydroxide in THF–MeOH (1 : 1) gave **6f** (83%).

Dimelamine **7a** (85%) was synthesized by reaction of **9** with excess of gly–gly ethyl ester in presence of DIPEA in THF. Hydrolysis of **6a** with sodium hydroxide in THF–MeOH (1 : 1) and coupling of L-alanine methyl ester, L-serine methyl ester or gly–gly ethyl ester using standard peptide coupling conditions (HATU, DIPEA in CH_2Cl_2) afforded **7b** (50%), **7c** (23%) and **8a** (68%), respectively.

Coupling of Boc-L-glu(OcHx)–OH with isopropyl amine using peptide coupling conditions (EDC, HOBT, DIPEA in $CHCl_3$) gave Boc-L-glu(OcHx)–NH*i*Pr (88%), which after deprotection with TFA–CH_2Cl_2 (1 : 1) was coupled with **6f** using standard peptide coupling conditions (EDC, HOBT, DIPEA in CH_2Cl_2) giving **7d** (48%). Dimelamine **7e** (66%) was obtained similarly to **7d** but using L-tyrosine methyl ester.

Fmoc-L-gln(Trt)–L-ser(O*t*Bu)–OMe was prepared by coupling of Fmoc-L-gln(Trt)–OH and L-ser(O*t*Bu)–OMe with HBTU and DIPEA in acetonitrile. Successive Fmoc cleavage with diethylamine gave L-gln(Trt)–L-ser(O*t*Bu)–OMe (90%). Coupling of **6f** with L-gln(Trt)–L-ser(O*t*Bu)–OMe using standard peptide coupling conditions (EDC, HOBT, DIPEA in CH_2Cl_2) afforded **8b** (45%).

The detailed experimental procedures and compound characterization can be found in the electronic supplementary information.

The double rosette formation with dimelamines **1**–**8** and various BAR/CYA was confirmed by ^{1}H NMR spectroscopy.[12] The ^{1}H NMR spectra of assemblies **1**–**8**$_3$·$(BAR)_6$ exhibit diagnostic signals between δ = 14.5–14.0 ppm (H_a), 13.5–13.0 ppm (H_b), 8.5–8.0 ppm (H_c), 7.4–7.2 ppm (H_d), 7.0–6.5 ppm ($H_{e,f}$), and *ca.* 6.0 ppm (H_h) (Fig. 3a). ^{1}H NMR spectra of assemblies **1**–**8**$_3$·$(CYA)_6$ exhibit diagnostic signals between δ = 15.0–14.0 ppm (H_a), 14.0–13.0 ppm (H_b), 8.8–8.3 ppm (H_c), 7.7–7.3 ppm (H_d), 7.2–6.6 ppm ($H_{e,f}$), and *ca.* 6.0 ppm (H_h) (Fig. 3b). Formation of assemblies **1**–**8**$_3$·$(BAR/CYA)_6$ was quantified by integration of the appropriate ^{1}H NMR signals[13] and confirmed by MALDI-TOF mass spectrometry using the Ag^+-labelling technique.[5b,14]

Thermodynamic stability of assemblies with alkyl (1a–c), aminoalkyl (2a–g), ureido (3) and pyridyl (4a–c) functionalities. The spontaneous assembly of double rosettes in apolar solvents is an enthalpy driven process that involves the cooperative formation of 36 hydrogen bonds. The change in entropy is unfavorable, because upon assembly formation the translational and rotational degrees of freedom of 9 molecular components are severely reduced.[15] The formation of hydrogen bonds favors the assembly of the double rosettes enthalpically. Hydrogen-bonding solvents lower this enthalpy, causing double rosettes eventually to dissociate. The amount of polar solvent required for dissociation can be taken as a measure for the stability of the double rosettes.[16]

The effect of linear (**1a**) and branched (**1b**–**c**) alkyl functionalities on the thermodynamic stability of the corresponding double rosettes was investigated by CD spectroscopy. Double rosettes with chiral building blocks display very intense and characteristic CD spectra[5a,8,17] that are not observed for the individual components. The CD signal is therefore a direct measure of assembly formation. Since calix[4]arene dimelamines **1a**–**c** are not chiral, (*R*)-PhEtCYA was used as chiral building block. For the CD titration experiments the percentage of methanol in chloroform was increased while the total concentration of dimelamine and of (*R*)-PhEtCYA was kept constant at 3 mM and 6 mM, respectively. Under these conditions the maximum concentration of double rosette assemblies is 1 mM. Unless mentioned otherwise, CD titrations were started with rosette solutions in neat $CHCl_3$, and subsequently the amount of MeOH was increased up to MeOH–$CHCl_3$ (1:1). The parameter $\chi_{polar\ solvent}$ was used to quantify the thermodynamic stability of double rosette assemblies. $\chi_{polar\ solvent}$ is defined as the percentage of polar solvent in chloroform at which 50% of the assembly is still intact.

Fig. 4 shows the results of CD titration experiments with assemblies **1a**–**c**$_3$·$((R)\text{-PhEtCYA})_6$. At MeOH–$CHCl_3$ (1 : 1) the double rosette **1a**$_3$·$((R)\text{-PhEtCYA})_6$ is still present for 58%. Though χ_{MeOH} lies beyond the range of the titration experiment a χ_{MeOH} of 60% was estimated (see Fig. 4). The branched isopropyl functionalities in **1b**$_3$·$((R)\text{-PhEtCYA})_6$ resulted in less stable double rosettes (χ_{MeOH} = 17%). Further branching by *tert*-butyl moieties in **1c**$_3$·$((R)\text{-PhEtCYA})_6$ gave a further decrease of stability (χ_{MeOH} = 7%). The decrease in thermodynamic stability is obviously due to a larger steric strain of the rosette platforms induced by the more voluminous branched alkyl functionalities.

For the series of amino alkyl functionalized double rosette assemblies **2a**–**f**$_3$·$((R)\text{-PhEtCYA})_6$, no significant change in thermodynamic stability was observed when the length of the amino alkyl chain was increased from aminoethyl to aminoheptyl (Fig. 5). The χ_{MeOH} values are in the range of 39 to 48%. The amino group present in assemblies **2a**–**f**$_3$·$((R)\text{-PhEtCYA})_6$

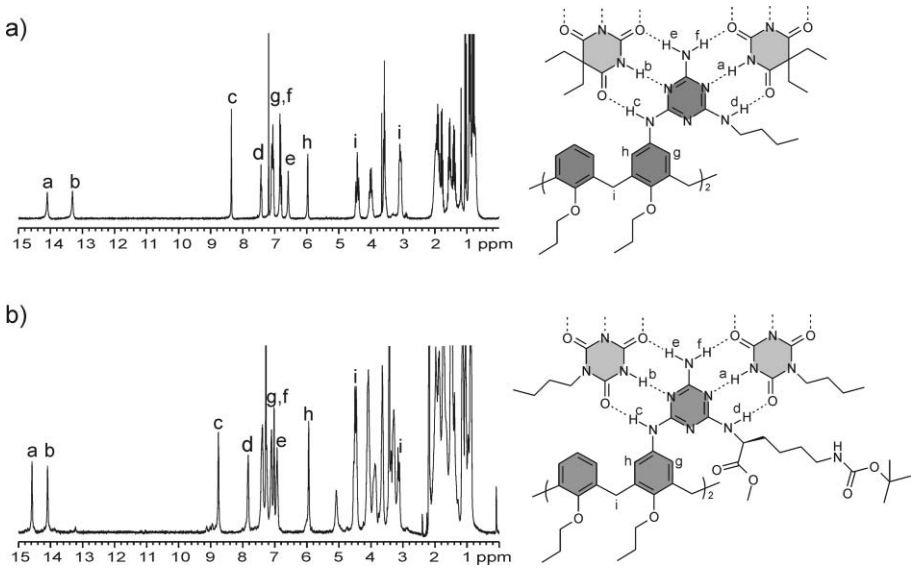

Fig. 3 ^{1}H NMR spectra of assembly (a) **1a**$_3$·$(DEB)_6$ and (b) **6d**$_3$·$(BuCYA)_6$. Spectra were recorded at 300 MHz in $CDCl_3$ at 298 K. (For clarity only the molecular structure of part of one rosette floor of the assemblies is shown).

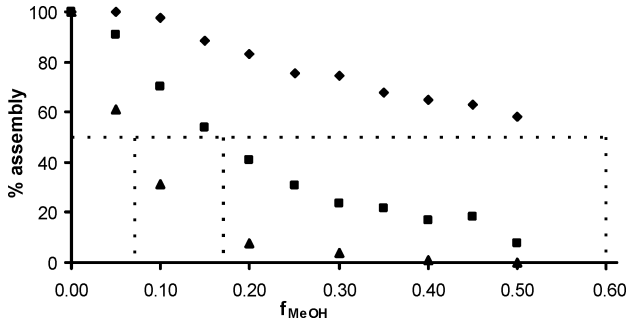

Fig. 4 CD titrations of ◆: **1a**$_3$·((*R*)-PhEtCYA)$_6$, ■: **1b**$_3$·((*R*)-PhEtCYA)$_6$, and ▲: **1c**$_3$·((*R*)-PhEtCYA)$_6$. Spectra were recorded in MeOH–$CHCl_3$ mixtures (f_{MeOH}) at 298 K. [**1a**–**c**] = 3 mM, [(*R*)-PhEtCYA$_6$] = 6 mM.

enhances the solubility in more polar solvents (mixtures) compared to double rosettes **1a**–**c**$_3$·((*R*)-PhEtCYA)$_6$, but it does not enhance the stability. When a CD titration with assembly **2e**$_3$·((*R*)-PhEtCYA)$_6$ was performed in MeOH–$CHCl_3$ mixtures ranging from neat chloroform to neat methanol (Fig. 5) a linear decrease of intact assemblies with increasing amount of methanol was found between ratios 1 : 9 and 8 : 2 (MeOH–$CHCl_3$). Above a ratio of 8 : 2, complete dissociation of double rosette **2e**$_3$·((*R*)-PhEtCYA)$_6$ was observed.

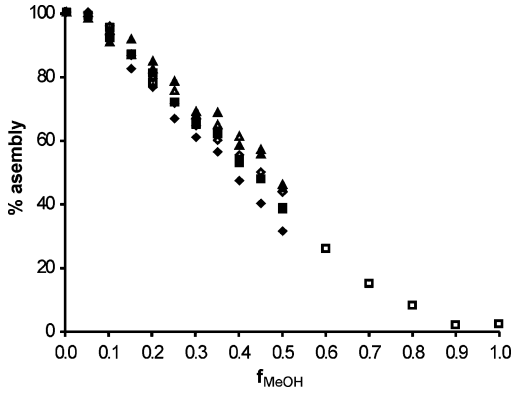

Fig. 5 CD titrations of ◆: **2a**$_3$·((*R*)-PhEtCYA)$_6$, ■: **2b**$_3$·((*R*)-PhEtCYA)$_6$, ▲: **2c**$_3$·((*R*)-PhEtCYA)$_6$, ◇: **2d**$_3$·((*R*)-PhEtCYA)$_6$, □: **2e**$_3$·((*R*)-PhEtCYA)$_6$, and Δ: **2f**$_3$·((*R*)-PhEtCYA)$_6$. Spectra were recorded in MeOH–$CHCl_3$ mixtures (f_{MeOH}) at 298 K. [**2a**–**f**] = 3 mM, [(*R*)-PhEtCYA$_6$] = 6 mM.

CD titrations with ureido functionalized double rosette **3**$_3$·((*R*)-PhEtCYA)$_6$ performed in MeOH–$CHCl_3$ mixtures ranging from neat methanol to chloroform gave a χ_{MeOH} of 82%. Thus, the ureido functionalities in **3**$_3$·((*R*)-PhEtCYA)$_6$ increase considerably the stability compared to assembly **1a**$_3$·((*R*)-PhEtCYA)$_6$ bearing butyl moieties. This increase is the result of a very rigid conformation adopted by the 2,2-dimethylpropyl side chain allowing the ureido moiety to fold back over the calix[4]arene aromatic rings and to form an extra hydrogen bond with one of the nitrogen atoms of the triazine ring (Fig. 6).[17]

For pyridyl functionalized assemblies **4a**–**c**$_3$·((*R*)-PhEtCYA)$_6$ a χ_{MeOH} of 53% was found, comparable to the stability of aminoalkyl funtionalized assemblies **2a**–**f**$_3$·((*R*)-PhEtCYA)$_6$.

In summary, branching of alkyl functionalities cause larger steric strain of the rosette platforms and decreases the thermodynamic stability. More polar aminoalkyl or pyridyl functionalities decrease the thermodynamic stability compared to *n*-alkyl functionalities but enhance the solubility in polar solvents (mixtures). The double rosette assembly with ureido functionalities is the most stable due to the formation of extra hydrogen bonds of the ureido groups with the triazine rings.

Formation and thermodynamic stability of assemblies with carbohydrate moieties (5a–e). Carbohydrates are involved in a large variety of biological molecular recognition processes.[18] Therefore, the introduction of carbohydrate oligomers in double rosette assemblies is very interesting for the mimicking of natural recognition events. However, before studying the properties of these assemblies as receptors it is important to assess their thermodynamic stability.

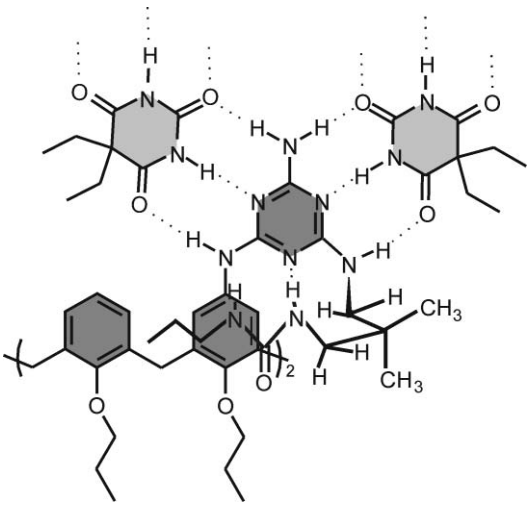

Fig. 6 Part of the molecular structure of assembly **3**$_3$·(DEB)$_6$ where the back folding of the ureido moieties is shown.[17]

Double rosette assemblies **5a**$_3$·(BuCYA)$_6$ and **5c**$_3$·(BuCYA)$_6$, bearing protected glucosyl and cellobiosyl moieties, respectively, are formed for 80% in $CDCl_3$ as estimated by ^{1}H NMR spectroscopy.[13] Furthermore, only one set of singlets was observed within the region from 13 to 15 ppm for both assemblies, indicating the presence of only one diastereomer in solution.[17b,c] CD spectroscopy revealed that both **5a**$_3$·(BuCYA)$_6$ and **5c**$_3$·(BuCYA)$_6$ exhibit *P*-helicity.

CD titration experiments with **5a**$_3$·(BuCYA)$_6$ in MeOH–$CHCl_3$ gave a χ_{MeOH} value of 18% (Table 1). Assembly **5c**$_3$·(BuCYA)$_6$ is formed in pure chloroform, but addition of methanol results in rapid dissociation. Free dimelamine **5c** exhibits a significant CD intensity induced by its 16 chiral centers that coincide with double rosette **5c**$_3$·(BuCYA)$_6$ but the CD spectrum differs in shape. The observed CD signals are the sum of the CD intensities attributed to free dimelamine **5c** and to assembly **5c**$_3$·(BuCYA)$_6$. CD titrations showed that above MeOH–$CHCl_3$ (2 : 8) the observed CD spectrum matches the spectrum of **5c**, indicating that assembly **5c**$_3$·(BuCYA)$_6$ is completely dissociated. CD titrations indicated that χ_{MeOH} is <5% for **5c**$_3$·(BuCYA)$_6$.

^{1}H NMR spectroscopy in chloroform indicated that assemblies **5b**$_3$·(BuCYA)$_6$ and **5d**$_3$·(BuCYA)$_6$, bearing unprotected glucosyl and cellobiosyl moieties, are formed for >95 and 76%, respectively. CD titrations with **5d**$_3$·(BuCYA)$_6$ were performed in a solvent mixture ranging from MeOH–$CHCl_3$ (2 : 8) (where 34% assembly is formed) to neat MeOH (χ_{MeOH} is <20%). As observed for CD titrations with **5c**$_3$·(BuCYA)$_6$, free **5d** also contributes significantly to the observed CD signal. Because the shape

Table 1 Thermodynamic stability for the self-assembly of double rosettes **5a**–**e**$_3$·(BuCYA)$_6$ in MeOH–$CHCl_3$ mixtures determined by CD titration experiments (298 K). The maximum possible concentration of intact assembly over the whole titration is 1.0 mM

R	Assembly	χ_{MeOH} (solvent range)
Glucopyranosyl(OAc)$_4$	**5a**$_3$·(BuCYA)$_6$	18% (0–50% MeOH)
Glucopyranosyl(OH)$_4$	**5b**$_3$·(BuCYA)$_6$	N.d.[a]
Cellobiosyl(OAc)$_7$	**5c**$_3$·(BuCYA)$_6$	<5% (0–50% MeOH)
Cellobiosylsyl(OH)$_7$	**5d**$_3$·(BuCYA)$_6$	<20% (20–100% MeOH)
Gulonyl	**5e**$_3$·(BuCYA)$_6$	10% (0–50% MeOH)

[a] Not determined.

of the CD spectra varies between free **5d** and **5d**$_3$·(BuCYA)$_6$ it is possible to quantify the double rosette formation. CD intensities at 260 nm were used because the assembly exhibit strong CD intensity at this wavelength, while the CD intensity for free **5d** is minimal. From these data $\Delta\varepsilon_{260}$ values of 147.1 and 0.4 l mol^{-1} cm^{-1} were calculated for **5d**$_3$·(BuCYA)$_6$ and free **5d**, respectively. In addition, **5d**$_3$·(BuCYA)$_6$ was formed for 25 and 7% in mixtures of MeOH–$CHCl_3$ in 3 : 7 and 4 : 6 volume ratio, respectively. At higher MeOH–$CHCl_3$ ratios, assembly **5d**$_3$·(BuCYA)$_6$ is not formed.

^{1}H NMR spectroscopy indicated that assembly **5e**$_3$·(BuCYA)$_6$, bearing L-gulose moieties, was formed for 65% in $CDCl_3$. This assembly forms the *M*-diastereomer. CD titration measurements in MeOH–$CHCl_3$ gave a χ_{MeOH} of 10% (Table 1).

Formation and thermodynamic stability of assemblies with amino acid functionalities (6a–f). For assembly (*P*)–**6a**$_3$·((*R*)-PhEtCYA)$_6$ a χ_{MeOH} value of 43% was obtained (Table 2). Dimelamine **6a** has the achiral amino acid Gly, thus (*R*)-PhEtCYA was used for the CD titration experiments to induce the formation of only one diastereomer.

Assembly **6b**$_3$·(BuCYA)$_6$, bearing alanine methyl ester moieties, is stable upon addition of 50% of MeOH (Fig. 7, Table 2). Further increase of the MeOH concentration was not possible due to solubility limitations. CD titrations with assembly **6b**$_3$·((*R*)-PhEtCY)$_6$ gave a χ_{MeOH} of 39%, a value comparable with that for **6a**$_3$·((*R*)-PhEtCYA)$_6$. These results indicate that the methyl side chain moiety of alanine does not interfere with the stability of assembly **6b**$_3$·(BuCYA)$_6$. Futhermore, assembly **6b**$_3$·(BuCYA)$_6$ is more stable than assembly **6a**$_3$·((*R*)-PhEtCYA)$_6$. It is possible that branching of the cyanurate side chain in (*R*)-PhEtCYA close to the rosette core causes more steric hindrance than BuCYA. CD titrations showed that assemblies **6c**$_3$·(BzCYA)$_6$, and **6d**$_3$·(BzCYA)$_6$, bearing L-methionine methyl ester and L-lysine(Boc) methyl ester moieties, are stable up to 50% of methanol (Table 2). Also, further increase of the methanol concentration was not possible due to solubility limitations. These results indicate that branching of the cyanurate side chain, as in (*R*)-PhEtCYA is indeed unfavorable. Furthermore, these results show that the methylsulfide and *tert*-butoxycarbonyl aminobutyl side chain functionalities of **6c** and **6d**, respectively, do not affect the stability of assemblies **6c**$_3$·(BzCYA)$_6$, and **6d**$_3$·(BzCYA)$_6$. CD titrations with **6d**$_3$·(BuCYA)$_6$ showed that this assembly is also stable in 50% of MeOH (Table 2). Fig. 7 clearly indicates that small differences in cyanurate side chain functionalities can decrease the stability of double rosette assemblies, while the effect of amino acid side chain functionalities at the calix[4]arene dimelamine units is almost negligible.

Table 2 Thermodynamic stability for the self-assembly of double rosettes **6a**–**f**$_3$·(BAR/CYA)$_6$ in MeOH–$CHCl_3$ mixtures determined by CD titration experiments (298 K). The maximum possible concentration of intact assembly over the whole titration is 1.0 mM

R	Assembly	χ_{MeOH} (solvent range)
Gly–OEt	**6a**$_3$·((*R*)-PhEtCYA)$_6$	43% (0–50% MeOH)
Ala–OMe	**6b**$_3$·(BuCYA)$_6$	Quantitative (0–50% MeOH)[a]
	6b$_3$·((*R*)-PhEtCYA)$_6$	39% (0–50% MeOH)
Met–OMe	**6c**$_3$·(BzCYA)$_6$	Quantitative (0–50% MeOH)[a]
Lys(Boc)–OMe	**6d**$_3$·(DEB)$_6$	3.2% (0–50% MeOH)
	6d$_3$·(BuCYA)$_6$	Quantitative (0–50% MeOH)[a]
	6d$_3$·(BzCYA)$_6$	Quantitative (0–50% MeOH)[a]
Lys–OMe	**6e**$_3$·(BuCYA)$_6$	49% (0–100% MeOH)
Lys(Boc)–OH	**6f**$_3$·(DEB)$_6$	No rosette
(*M*-Isomer)	**6f**$_3$·(BuCYA)$_6$	40% (0–100% MeOH)
	6f$_3$·((*R*)-PhEtCYA)$_6$	No rosette
	6f$_3$·((*S*)-PhEtCYA)$_6$	Rosette <15% in $CDCl_3$

[a] Assembly formation is quantitative over the whole solvent range.

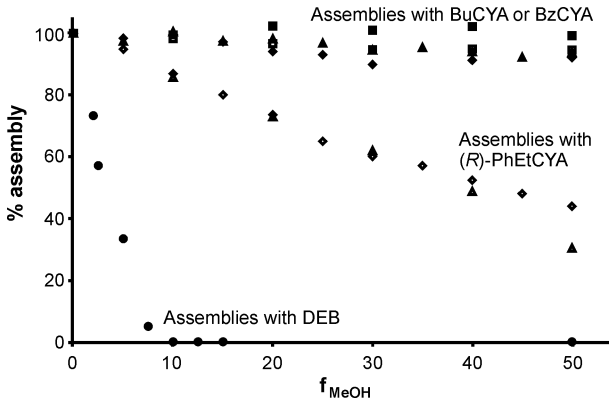

Fig. 7 CD titrations of assemblies **6a**$_3$·((*R*)-PhEtCYA)$_6$ (◇), **6b**$_3$·((*R*)-PhEtCYA)$_6$ (Δ), **6b**$_3$·(BuCYA)$_6$ (□), **6c**$_3$·(BzCYA)$_6$ (■), **6d**$_3$·(DEB)$_6$ (●), **6d**$_3$·(BuCYA)$_6$ (◆), and **6d**$_3$·(BzCYA)$_6$ (▲). Spectra were recorded in MeOH–$CHCl_3$ (f_{MeOH}) mixtures at 298 K where the maximum assembly concentration was kept constant (1.0 mM).

Previously, our group has reported[19] that the assembly of one melamine to one cyanurate (CYA) gives a complex that is much stronger than the complex between one melamine and one barbiturate (BAR) due to the higher acidity of the CYA. Association constants of 10^2 and 10^4 M^{-1} were reported for melamine–BAR and melamine–CYA, respectively. In agreement with this, we found a very low stability ($\chi_{MeOH} = 3.2\%$; Table 2) for assembly **6d**$_3$·(DEB)$_6$, formed with diethyl barbiturate instead of cyanurate derivatives.

For **6e**$_3$·(BuCYA)$_6$, bearing unprotected (side chain) L-lysine methyl ester moieties the χ_{MeOH} is 49% (Table 2). This indicates that the free ε-amino group of the lysine gives a less stable double rosette assembly **6e**$_3$·(BuCYA)$_6$ compared to **6d**$_3$·(BuCYA)$_6$ (formed quantitatively in 0–50% MeOH in $CHCl_3$ at 1 mM), in which the ε-amino group of the lysine is Boc-protected. For assembly **6f**$_3$·(BuCYA)$_6$, with free carboxylic acid groups the χ_{MeOH} is 40%. Assembly **6f**$_3$·(BuCYA)$_6$ is less stable than its methyl ester analogue **6d**$_3$·(BuCYA)$_6$. Assembly **6f**$_3$·(DEB)$_6$ was not formed at any ratio MeOH–$CHCl_3$ at 1.0 mM concentration, emphasizing the weaker association between melamine·BAR compared to melamine·CYA. Previous results indicate that the stability of double rosettes was mainly affected by the molecular structure of the cyanurates and not by the side chain functionality of the amino acid esters. Because dimelamine **6d** is bulkier than dimelamines **6e** and **6f**, charge or electronic influences of the ε-amino or carboxylic acid groups in **6e**$_3$·(BuCYA)$_6$ and **6f**$_3$·(BuCYA)$_6$, respectively, rather than steric hindrance seem to decrease their stability.

Chiral induction by the lysine group

Dimelamines **6b**, **6c**, **6d** and **6e**, having L-alanine methyl ester, L-methionine methyl ester, ε-*N*-Boc-L-lysine methyl ester or L-lysine methyl ester moieties, respectively, all induce (*P*)-helicity in the assembly formation. However, the CD spectrum observed for **6f**$_3$·(BuCYA)$_6$, bearing the L-lysine amino acid with a free carboxylic acid group, is inverted compared to the double rosettes **6b**–**e**$_3$·(DEB/CYA)$_6$ with the amino ester functionalities. This indicates that dimelamine **6f** induces (*M*)-helicity for the double rosette **6f**$_3$·(BuCYA)$_6$, even though the chirality of dimelamine **6f** (L-lys) is the same as of the other lysine functionalized dimelamine derivatives **6d** and **6e**.

The formation of assemblies **6f**$_3$·((*R*)-PhEtCYA)$_6$ and **6f**$_3$·((*S*)-PhEtCYA)$_6$ was studied to confirm that in all cases L-**6f** induces the *M*-helicity. Generally, when chiral dimelamines and chiral cyanurate derivatives have an opposite preference for induction of (*M*)- or (*P*)-helicity, the formation of double rosettes is not observed.[20,21] Assembly **6b**$_3$·((*R*)-PhEtCYA)$_6$ is only formed in the (*P*)-helical form, thus (*R*)-PhEtCYA induces only the (*P*)-helicity. ^{1}H NMR and CD spectroscopy studies indicate the

formation of the assembly **6f**$_3$·((*S*)-PhEtCYA)$_6$ with the (*M*)-helicity but assembly **6f**$_3$·((*R*)-PhEtCYA)$_6$ is not formed. Thus, L-**6f** induces only the (*M*)-helicity.

It is known that the induction of helicity by amino acid residues could depend on the solvent polarity and on the pH.[22] Though it is difficult to explain this change in helicity it is likely that differences in polarity between the different lysine moieties of **6d**, **6e** and **6f** are playing a role. The complete inversion of helicity as observed for **6f**$_3$·(BuCYA)$_6$, compared to other amino acid functionalized assemblies, indicates that small structural changes within the building blocks could largely affect the structure of the assembly.

Formation and thermodynamic stability of assemblies with di-(7a–e) and tripeptide (8a–b) functionalities. ^{1}H NMR spectroscopy showed that assemblies **7a**$_3$·((*R*)-PhEtCYA)$_6$, **7b**$_3$·(BuCYA)$_6$ and **7c**$_3$·(BuCYA)$_6$, bearing gly–gly–OEt, gly–L-ala–OMe and gly–L-ser–OMe functionalities, respectively, were formed quantitatively in $CDCl_3$, while **7d**$_3$·(BuCYA)$_6$ and **7e**$_3$·(BuCYA)$_6$, bearing L-lys(Boc)-L-glu(OcHx)-NH*i*Pr and L-lys(Boc)–L-tyr–OMe functionalities were formed only for 84 and 65%, respectively.

CD titration experiments were performed with **7a**$_3$·((*R*)-PhEtCYA)$_6$, **7b**$_3$·(BuCYA)$_6$, **7d**$_3$·(BuCYA)$_6$ and **7e**$_3$·(BuCYA)$_6$ in MeOH–$CHCl_3$ (Table 3). Because dipeptide functionalized dimelamines **7a–e** are soluble in methanol, titrations could be performed from neat chloroform to neat methanol. For these dipeptide functionalized double rosettes, it was found that an increase of the ratio MeOH–$CHCl_3$ leads to the dissociation of the double rosettes. Assembly **7a**$_3$·((*R*)-PhEtCYA)$_6$ (χ_{MeOH} = 25%) is less stable than the corresponding (mono) glycine derivative **6a**$_3$·((*R*)-PhEtCYA)$_6$ (χ_{MeOH} = 43%; Table 2). These results indicate that the presence of a dipeptide instead of a single amino acid decreases severely the stability of the assembly.

Assembly **7b**$_3$·(BuCYA)$_6$ with gly–L-ala functionalities (χ_{MeOH} = 50%) was formed for 50% in MeOH–$CHCl_3$ (1 : 1), while **6b**$_3$·(BuCYA)$_6$, bearing only L-ala, was formed quantitatively (Table 2). Furthermore, the double rosettes **7d**$_3$·(BuCYA)$_6$ and **7e**$_3$·(BuCYA)$_6$, with bulkier dipeptides are less stable (χ_{MeOH} values of 7 and 8%, respectively) than **7b**$_3$·(BuCYA)$_6$. Because the lysine at the first position did not affect the formation of **6d**$_3$·(BuCYA)$_6$ (formed quantitatively in MeOH–$CHCl_3$ (1 : 1); Table 2), these results indicate that bulkier amino acids in the second position decrease the stability in MeOH–$CHCl_3$ solvent mixtures. However, above MeOH–$CHCl_3$ (2 : 8) no further dissociation of **7d**$_3$·(BuCYA)$_6$ and **7e**$_3$·(BuCYA)$_6$ was observed as it can be seen by CD titrations. The percentage intact assemblies for **7d**$_3$·(BuCYA)$_6$ and **7e**$_3$·(BuCYA)$_6$ remained around 20% (Fig. 8), even in pure methanol!

For tripeptide functionalized double rosettes, ^{1}H NMR spectroscopy indicated that the double rosette assembly **8a**$_3$·((*R*)-PhEtCYA)$_6$, bearing gly–gly–gly–OEt moieties, was formed quantitatively in chloroform. CD titrations gave χ_{MeOH} = 23% which is similar to **7a**$_3$·((*R*)-PhEtCYA)$_6$ bearing the corresponding dipeptide gly–gly–OEt. This indicates that the introduction of the third amino acid does not further decrease the stability. The ^{1}H NMR spectrum of the assembly **8b**$_3$·(BuCYA)$_6$, bearing L-lys(Boc)–L-gln(Trt)–L-ser(O*t*Bu)–OMe moieties showed the diagnostic signals for double rosette formation in chloroform. However, it was not possible to quantify the rosette formation due to peak broadening in the ^{1}H NMR spectrum. To estimate the double rosette formation, the CD signal (at 300 nm) obtained for **8b**$_3$·(BuCYA)$_6$ in chloroform was compared with the intensity of the CD signal of **6d**$_3$·(BuCYA)$_6$ in the same solvent. This resulted in an estimated formation of **8b**$_3$·(BuCYA)$_6$ of 40% in chloroform. CD titrations showed that increased polarity led also here to dissociation. Assembly **8b**$_3$·(BuCYA)$_6$ was formed about 15–20% in neat MeOH (Table 3) which is comparable with assemblies **7d**$_3$·(BuCYA)$_6$ and **7e**$_3$·(BuCYA)$_6$ (20% of rosette formation also in neat MeOH). It seems that bulky and polar amino acids at the second and possibly at the third position increase the stability of double rosettes in *neat* MeOH, contrary to what is observed for MeOH–$CHCl_3$ mixtures with high content of $CDCl_3$. These could suggest that with larger and bulkier peptide functionalities at the assemblies solvophobic interactions similar to the hydrophobic effects for the self-assembly of amphiphilic molecules in water, might start to play a role in the self-assembly process.

In summary, amino acids at the first position of the peptide functionalities do not affect the formation of double rosettes at 1 mM concentration in MeOH–$CHCl_3$ solvent mixtures, while amino acids at the second position in di- and tripeptide functionalities decrease the stability of double rosette assemblies in the same solvent mixtures. This decrease in stability becomes larger when more bulky amino acids are used in the second position. Interestingly, it seems that the introduction of the third amino acid hardly affects the stability of double rosettes when compared with the dipeptides. Surprisingly, in neat MeOH assembly formation (*ca.* 20%) is only observed when bulky and polar amino acids are present at the second (and third) position.

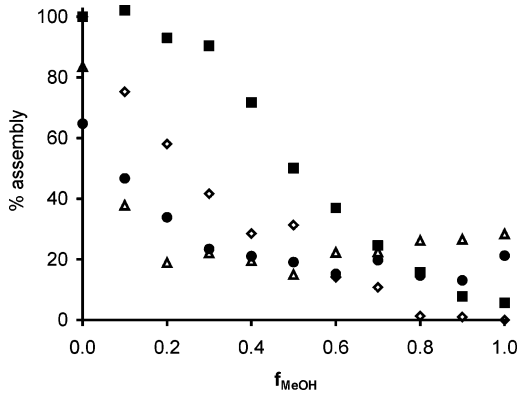

Fig. 8 CD titrations of assemblies **7a**$_3$·((*R*)-PhEtCYA)$_6$ (■), **7b**$_3$·(BuCYA)$_6$ (◊), **7d**$_3$·(BuCYA)$_6$ (Δ) and **7e**$_3$·(BuCYA)$_6$ (●). Spectra were recorded in MeOH–$CHCl_3$ (f_{MeOH}) mixtures at 298 K where the maximum assembly concentration was kept constant (1.0 mM).

Table 3 Thermodynamic stability for the self-assembly of double rosettes **7a**–**e**$_3$·((*R*)-PhEtCYA/BuCYA)$_6$ and **8a**–**b**$_3$·((*R*)-PhEtCYA/BuCYA)$_6$ in MeOH–$CHCl_3$ mixtures determined by CD titration experiments (298 K). The maximum possible concentration of intact assembly over the whole titration is 1.0 mM

R	Assembly	χ_{MeOH} (solvent range)
Gly–gly–OEt	**7a**$_3$·((*R*)-PhEtCYA)$_6$	25% (0–100% MeOH)[a]
Gly–L-ala–OMe	**7b**$_3$·(BuCYA)$_6$	50% (0–100% MeOH)[a]
Gly–L-ser–OMe	**7c**$_3$·(BuCYA)$_6$	N.d.[b]
L-Lys(Boc)–L-glu(OcHx)–NH*i*Pr	**7d**$_3$·(BuCYA)$_6$	7% (0–100% MeOH)[a]
L-Lys(Boc)–L-tyr–OMe	**7e**$_3$·(BuCYA)$_6$	8% (20–100% MeOH)[a]
Gly–gly–gly–OEt	**8a**$_3$·((*R*)–PhEtCYA)$_6$	23% (0–100% MeOH)[a]
L-Lys(Boc)–L-gln(Trt)–ser(O*t*Bu)–OMe	**8b**$_3$·(BuCYA)$_6$	Rosette formation *ca.* 40% in $CDCl_3$

[a] CD titrations were performed from neat $CHCl_3$ to neat MeOH due to the increased solubility of dimelamines **7** and **8** in methanol. [b] Not determined.

Conclusions

The results shown in here demonstrate that noncovalent hydrogen-bonded double rosettes with different functionalities in the building blocks can be formed in MeOH–$CHCl_3$ solvent mixtures. In general, increase of the solvent polarity leads to destabilization of the assemblies.

Furthermore, the functionalities strongly influence the stability of the double rosettes. Steric hindrance close to the rosette platform exerted by the functional groups of the building blocks decreases the stability. Aminoalkyl groups decrease the stability compared to *n*-alkyl functionalities. For linear aminoalkyl groups, it was observed that the chain length does not affect the stability. The stability of the double rosettes bearing pyridyl groups is comparable to the stabilities of assemblies with aminoalkyl groups. The ureido functionalized double rosette is the most stable.

Double rosettes with protected glucosyl and cellobiosyl moieties are also formed quantitative in neat chloroform, while assemblies with unprotected glucosyl and cellobiosyl moieties are formed for only *ca.* 80%. Carbohydrate moieties lead to a dramatic decrease in stability of double rosettes in polar solvents when compared to double rosettes having alkyl, aminoalkyl, pyridyl or ureido moieties.

Double rosettes with amino acid or peptide functionalities are more stable than double rosettes with carbohydrate moieties in polar solvents. The stability of double rosettes with different amino acid functionalities in polar solvents strongly depends on the barbiturate or cyanurate derivative. In all cases, assemblies with DEB are less stable than those with cyanurates. Assemblies of amino acid ester functionalized dimelamines **6a**–**d** with BuCYA or BzCYA are stable up to at least 50% of methanol in chloroform, while double rosettes with the more bulky branched (*R*)-PhEtCYA have χ_{MeOH} values of 40%. Assemblies with different lysine derivatives showed that free amino groups or free carboxylic acid groups within the assembly decrease the stability, probably due to ionic or electronic influences.

In apolar solvents, di- and tripeptide peptide functionalized assemblies are less stable compared to single amino acid functionalized assemblies. Amino acids at the first position of the peptide functionalities do not seem to affect the stability of double rosettes (at 1 mM), while amino acids at the second position decrease the stability of double rosette assemblies. This decrease in stability becomes larger when bulkier amino acids are present in the second position. The introduction of a third amino acid hardly influences the stability of the double rosettes.

Assembly formation in neat MeOH is observed only when bulky amino acids are present at the second (and third) position. This would indicate that the introduction of larger and/or bulkier peptides might stabilize double rosettes in polar solvents. This behavior is important for host–guest recognition in aqueous solvents.

Overall, the large range of functionalities that can be introduced on the rosette platform allows a large molecular diversity. This is useful to generate hydrogen-bonded receptor assemblies that resemble the natural antibodies. Introduction of large diverse peptides to the double rosettes seems therefore especially attractive because they might mimic the binding sites of these natural receptors. Recently we showed that it is possible to form double rosettes also in bilayer membranes.[23] The stability of the double rosettes is larger in the bilayer membranes compared to polar solutions. Efforts to integrate the hydrogen-bonded assemblies studied here as bilayer membrane receptors are currently ongoing in our laboratory.

Acknowledgements

Dr M. G. J. ten Cate and Dr M. Crego-Calama acknowledge the Technology Foundation of the Netherlands (CW-STW) and Royal Netherlands Academy of Arts and Science (KNAW) for financial support.

References

1 (*a*) R. Fiammengo, M. Crego-Calama and D. N. Reinhoudt, *Curr. Opin. Chem. Biol.*, 2001, **5**, 660–673; (*b*) M. Crego-Calama and D. N. Reinhoudt, *Science*, 2002, **295**, 2403–2407.
2 G. M. Whitesides, E. E. Simanek, J. P. Mathias, C. T. Seto, D. N. Shin, M. Mammen and D. M. Gordon, *Acc. Chem. Res.*, 1995, **28**, 37–44.
3 (*a*) E. Benjamini, G. Sunshine, S. Leskowitz, *Immunology, A Short Course, 3rd edn*, Wiley, New York, 1996; (*b*) L. Stryer, *Biochemistry, 4th edn*, Freeman and Company: New York, 1995.
4 P. Timmerman and D. N. Reinhoudt, *Adv. Mater.*, 1999, **11**, 71–74.
5 (*a*) R. H. Vreekamp, R. H. Van Duynhoven, M. Hubert, W. Verboom and D. N. Reinhoudt, *Angew. Chem., Int. Ed.*, 1996, **35**, 1215–1218; (*b*) P. Timmerman, K. A. Jollife, M. Crego-Calama, J. L. Weidmann, L. J. Prins, F. Cardullo, B. H. M. Snellink-Ruel, R. H. Fokkens, N. M. M. Nibbering, S. Shinkai and D. N. Reinhoudt, *Chem. Eur. J.*, 2000, **6**, 4104–4115.
6 J. M. C. A. Kerckhoffs, M. Crego-Calama, I. Luyten, P. Timmerman and D. N. Reinhoudt, *Org. Lett.*, 2000, **2**, 4121–4124.
7 (*a*) C. T. Seto and G. M. Whitesides, *J. Am. Chem. Soc.*, 1990, **112**, 6409–6411; (*b*) J. A. Zerkowski, C. T. Seto, D. A. Wierdo and G. M. Whitesides, *J. Am. Chem. Soc.*, 1990, **112**, 9025–9026.
8 P. Timmerman, R. H. Vreekamp, R. Hulst, W. Verboom, D. N. Reinhoudt, K. Risannen, K. A. Udachin and J. Ripmeester, *Chem. Eur. J.*, 1997, **3**, 1823–1832.
9 J. M. C. A. Kerckhoffs, M. Crego-Calama, I. Luyten, P. Timmerman and D. N. Reinhoudt, *Org. Lett.*, 2000, **2**, 4121–4124.
10 T. Ishi-i, M. Crego-Calama, P. Timmerman, D. N. Reinhoudt and S. Shinkai, *J. Am. Chem. Soc.*, 2002, **124**, 14631–14641.
11 (*a*) I. Yamamoto, K. Fukui, S. Yamamoto, K. Ohta and K. Matsuzaki, *Synthesis*, 1985, 686–688; (*b*) H. Ogura and H. Takahashi, *Heterocycles*, 1982, 87–90; (*c*) G. V. Oshovsky, W. Verboom, R. H. Fokkens and D. N. Reinhoudt, *Chem. Eur. J.*, 2004, **10**, 2739–2748.
12 (*a*) P. Timmerman and L. J. Prins, *Eur. J. Org. Chem.*, 2001, **17**, 3191–3205; (*b*) D. N. Reinhoudt, P. Timmerman, F. Cardullo, M. Crego-Calama, *NATO Science Series C*, vol 257, ed. R. Ungaro, E. Dalcanale, Kluwer Academic Publishers, Dordrecht, 1999; pp. 181–195.
13 The percentage of assembly was determined by comparison of the H_a + H_b intensity with the $ArCH_2Ar$ of the calix[4]arene part. Assembly $\mathbf{1a}_3\cdot(DEB)_6$ is used as standard, for which this ratio was arbitrarily set to 100%.
14 K. A. Jolliffe, M. Crego-Calama, R. Fokkens, N. M. M. Nibbering, P. Timmerman and D. N. Reinhoudt, *Angew. Chem., Int. Ed.*, 1998, **37**, 1247–1251.
15 Detailed analyses of energetic parameters are described in M. G. J. Ten Cate, J. Huskens, M. Crego-Calama and D. N. Reinhoudt, *Chem. Eur. J.*, 2004, **10**, 3632–3639.
16 M. Mammen, E. E. Simanek and G. M. Whitesides, *J. Am. Chem. Soc.*, 1996, **118**, 12614–12623.
17 (*a*) L. J. Prins, K. A. Jolliffe, R. Hulst, P. Timmerman and D. N. Reinhoudt, *J. Am. Chem. Soc.*, 2000, **122**, 3617–3627; (*b*) L. J. Prins, J. Huskens, F. De Jong, P. Timmerman and D. N. Reinhoudt, *Nature*, 1999, **398**, 498–502; (*c*) L. J. Prins, F. De Jong, P. Timmerman and D. N. Reinhoudt, *Nature*, 2000, **408**, 181–184.
18 (*a*) A. Varki, *Glycobiology*, 1993, **3**, 97–130; (*b*) R. A. Dwek, *Chem. Rev.*, 1996, **96**, 683–720; (*c*) M. Mammen, S.-K. Choi and G. M. Whitesides, *Angew. Chem., Int. Ed.*, 1998, **37**, 2754–2794.
19 A. G. Bielejewska, C. E. Marjo, L. J. Prins, P. Timmerman, F. De Jong and D. N. Reinhoudt, *J. Am. Chem. Soc.*, 2001, **123**, 7518–7533.
20 L. J. Prins, *Non-Covalent Synthesis of Chiral Hydrogen-Bonded Assemblies*, University of Twente, Enschede, The Netherlands, ISBN 90-365-1627-7, 2001.
21 Occasionally, double rosette formation could be observed with ^1H NMR spectroscopy, but these assemblies are hardly CD active because either the opposite chirality inducing components strongly affect the orientation of the chromophores responsible for the CD activity or coincidentally cause opposite CD activity of identical intensity.
22 K. K. L. Cheuk, J. W. Y. Lam, L. M. Lai, Y. Dong and B. Z. Tang, *Macromolecules*, 2003, **36**, 9752–9762.
23 M. G. J. Ten Cate, M. Crego-Calama and D. N. Reinhoudt, *J. Am. Chem. Soc.*, 2004, **126**, 10840–10841.